Spin Relaxation of Atomic Hydrogen in CaF_2: Evidence for Local Modes*

D. W. FELDMAN, J. G. CASTLE, JR., AND J. MURPHY
Westinghouse Research Laboratories, Pittsburgh, Pennsylvania
(Received 16 December 1964)

The spin-lattice relaxation time T_1 of atomic hydrogen in calcium fluoride has been measured at 3 kOe and at temperatures from 2.1 to 165°K. The values of T_1 can be expressed by

$$1/T_1 = BT + C(T/\theta)^7 J_6(\theta/T) + D_H \exp(-T_H/T),$$

where $B=0.028$ sec^{-1}°K^{-1}, $C=2.7\times10^4$ sec^{-1}, and $D=9\times10^6$ sec^{-1}. The characteristic temperatures are: $\theta=474$°K and $T_H=850\pm60$°K. The temperature dependence of the first two terms is consistent with the usual direct and Raman processes, but their relative magnitudes are not well understood. Similar measurements have been made on atomic deuterium centers. The relaxation data for deuterium centers can be accurately fitted by an expression of the above form in which: there is an additional term due to cross relaxation; B, C, and θ have the same values; and $D_D=8\times10^5$ sec^{-1} and $T_D=640\pm80$°K. The characteristic temperatures of 850 and 640°K are interpreted in terms of local modes which involve the motion of the interstitial hydrogen and deuterium atoms with respect to neighboring fluorines. The basis for this identification is discussed in terms of Feynman diagrams.

I. INTRODUCTION

THE atomic-hydrogen center in calcium fluoride has been studied in some detail.[1,2] On the basis of its electron-spin resonance and electron nuclear double-resonance (ENDOR) spectra, Hall and Schumacher[1] concluded that the center consists of a neutral hydrogen atom occupying an interstitial site at the center of a cube of eight fluorine ions. The hydrogen center has an isotropic g value nearly equal to that of the free atom. The well-resolved hyperfine spectrum, due both to the proton and to nearby fluorines, is consistent with an electronic ground state which is quite similar to that of the free hydrogen atom. No detailed crystal-field calculations on this center have been published. There have been no reports of optical spectra directly correlated with the spin concentration of H^0.

Klemens has suggested[3] that local modes of vibration at a defect site could dominate spin-lattice relaxation in certain cases. Local modes have been observed optically for substitutional H^- and D^- in calcium fluoride[4] and for substitutional H^- in alkali halides.[5] No direct evidence exists for local modes associated with interstitial H^0 in calcium fluoride. However, the small mass of the proton and the size of the hydrogen relative to the space in the fluorine cage suggest that some vibration should occur at frequencies well above the allowed bands for the normal CaF_2 lattice and therefore that local modes should exist.[6]

It is the purpose of this paper to present experimental evidence on the atomic-hydrogen and atomic-deuterium centers in calcium fluoride in the form of spin-relaxation results and to suggest an interpretation in terms of local modes.

II. THEORETICAL CONSIDERATIONS

Before considering the possible role of local modes in spin-lattice relaxation we will briefly summarize the usual theory that has been treated in detail elsewhere.[7–9] After the summary, we will outline the changes expected in spin relaxation when the spin is localized near a light-mass defect.

Logical completeness in the summary will be aided by the introduction of diagrams. A particularly descriptive presentation of spin-lattice relaxation processes is one that makes use of diagrams analogous to those developed by Feynman[10] for quantum electrodynamics. It is felt that this approach is sufficiently unfamiliar in the present connection to warrant some clarification.

A. Relaxation Diagrams

In the notation of quantum field theory, the spin-lattice interaction Hamiltonian can be written as

$$\mathcal{H}' = \sum_{ij} c_{ij} \Psi_i^\dagger \Psi_j \phi(a,a^\dagger) + \sum_{ij} c_{ij}' \Psi_j^\dagger \Psi_i \phi(a,a^\dagger), \quad (1)$$

where $\phi(a,a^\dagger)$ is a function of phonon annihilation operators (a) and phonon creation operators ($a^\dagger$), Ψ_j (or $\Psi_j^\dagger$) destroys (or creates) an electron in the state j, and c_{ij} are numerical coefficients.

Given the interaction (1), we can represent diagrammatically phonon absorption, emission, and scattering

* This work was supported in part by the U. S. Air Force Cambridge Research Laboratories.

[1] J. L. Hall and R. T. Schumacher, Phys. Rev. **127**, 1892 (1962).
[2] H. Blum and G. B. Benedek, Bull. Am. Phys. Soc. **8**, 619 (1963).
[3] P. G. Klemens, Phys. Rev. **125**, 1795 (1962).
[4] W. Hayes, G. D. Jones, R. J. Elliott, and C. T. Sennett, in *Proceedings of the Conference on Lattice Dynamics, Copenhagen 1963* (Pergamon Press, Inc., New York, 1964), p. 475.
[5] Akiyoshi Mitsushi and Hiroshi Yoshinoga, J. Phys. Soc. Japan **18**, 321 (1963).
[6] E. W. Montroll and R. B. Potts, Phys. Rev. **100**, 525 (1955) and P. G. Dawber and R. J. Elliott, Proc. Roy. Soc. (London) **A273**, 222 (1963).
[7] J. H. Van Vleck, Phys. Rev. **57**, 426 (1940).
[8] R. Orbach, Proc. Roy. Soc. (London) **A264**, 458 (1961).
[9] J. W. Culvahouse, W. P. Unruh, and D. K. Brice, Phys. Rev. **129**, 2430 (1963).
[10] R. P. Feynman, Phys. Rev. **74**, 939 (1948).

processes in all orders of perturbation theory. For processes involving the emission or absorption of single phonons, the relevant part of $\phi(a,a^\dagger)$ is $\sum_k b_k a_k$ where b_k is a number and the sum is over all lattice modes. The direct relaxation processes[7] are calculated by using this part of $\phi(a,a^\dagger)$ in Eq. (1) taken to first order.

For direct processes, we represent each term in the first and second sums of Eq. (1) by the diagram shown in Figs. 1(a) and 1(b), respectively. In all diagrams, we use the convention of time increasing in the upward direction, so that all lines converging on a vertex from below denote states in which quanta are destroyed and those lines diverging upward from a vertex, quanta created in the interaction. Wavy lines indicate electronic states and straight lines, lattice states. Figure 1(a) represents the destruction of one phonon in state k and one electron in state j and the creation of one electron in state i. The inverse transition is shown in Fig. 1(b). Relaxation occurs at a rate determined by the appropriate sum of the transition probabilities from both Figs. 1(a) and 1(b). In the remaining discussion, diagrams will be shown corresponding to one transition only. The inclusion of the inverse transitions for the calculation of each case is to be understood.

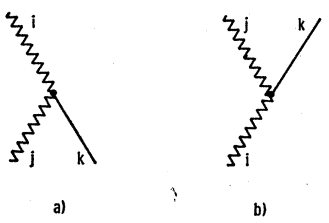

FIG. 1. Diagrams used in first-order perturbation calculation of relaxation processes arising from a spin-lattice interaction which is linear in strain. The two diagrams correspond to the two terms of Eq. (1) for the case discussed. Symbolism is discussed in the text.

For simplicity and aptness to the hydrogen atom, we will restrict this discussion of relaxation to electronic systems having an $S=\frac{1}{2}$ ground state and no other states within the frequency range of the phonon spectrum. For these cases, all possible first-order spin-lattice interactions which are linear in the strain are represented by Fig. 1 where the symbols i and j correspond to $M_s=\pm\frac{1}{2}$ and energy conservation requires that ω_k equal the Larmor frequency, ω_z.

After the populations of the states i and j are disturbed from their thermal-equilibrium values, relaxation takes place by emission and absorption of resonant phonons, as indicated in Fig. 1. To calculate the relaxation-time constant characteristic of a direct process as a function of field and temperature, it is necessary to have a specific model for the interaction coefficients $c_{ij}b_k$, including the frequency dependence of the effective local strain, and for the distribution of the lattice modes.

Any real relaxation involves anharmonic motions of the surrounding atoms and diagrams can be used to represent the calculation of the relaxation time by a perturbation expansion in terms of harmonic modes of the lattice. A direct process involving relaxation by

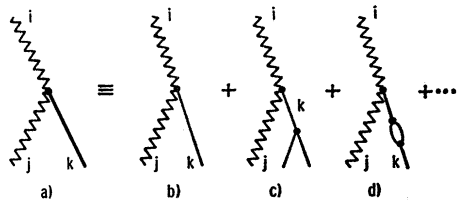

FIG. 2. Diagram representing spin-lattice interactions linear in strain generated in the anharmonic lattice. The heavy line signifies a broadened mode. The expansion assumes broadening by the cubic anharmonicity of the lattice.

nearly harmonic motions is represented in Fig. 2, where the heavy straight line in 2(a) stands for an eigenstate of the anharmonic lattice and the lighter straight lines in 2(b), 2(c), and 2(d) represent modes of the harmonic lattice. Let us assume that the coupling that limits the lifetime of phonons is the cubic anharmonicity of the lattice.[11] Part of the expansion in terms of the cubic anharmonicity is illustrated in Figs. 2(b), 2(c), and 2(d). Notice that the usual direct process with phonons [Fig. 1(a)] is just the zeroth-order term [Fig. 2(b)] in this expansion. The second term, 2(c), represents the effect to first order of the cubic anharmonicity and is expected to be much smaller than the first term for most real lattices.

Higher-order processes of relaxation can also be represented diagrammatically. For example, the inelastic scattering of phonons involving the spin-lattice coupling quadratic in the strain is shown in Fig. 3. Another two-phonon process involving the linear coupling in second order is shown in Fig. 4. The processes indicated in Figs. 3(b) and 4(b) are the only ones usually considered as the Raman processes. Before discussing them, we will pick a specific model and predict the temperature dependence for the direct process.

B. Relaxation in the Unperturbed Lattice

Relaxation is usually pictured as proceeding via phonons which produce strain at the spin site proportional to their frequency and to their amplitude. The lattice is assumed to have an isotropic Debye spectrum.

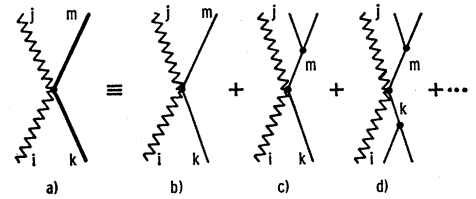

FIG. 3. Diagram representing spin-lattice interactions quadratic in strain. The symbolism is the same as in Fig. 2. The sum over (c) includes application of the cubic anharmonicity prior to the spin-lattice interaction.

[11] P. G. Klemens in *Solid State Physics*, edited by F. Seitz and D. Turnbull (Academic Press Inc., New York, 1958), Vol. 7, p. 1.

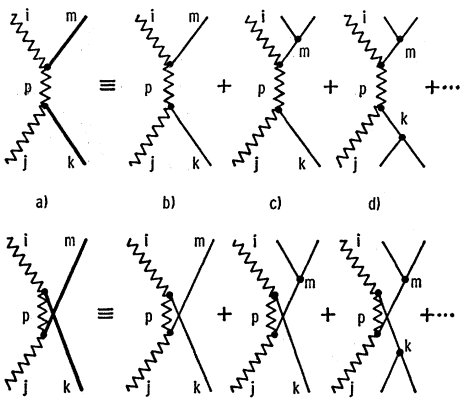

FIG. 4. Diagrams used in the second-order perturbation calculations for spin-lattice interactions linear in strain. The symbolism is the same as in Fig. 2. The sum over (c) includes the application of the cubic anharmonicity prior to the spin-lattice interaction.

The direct process involves long-wavelength phonons for which this model is quite accurate. The reciprocal of the relaxation time is proportional to the average number of resonant phonons, as indicated for process 2(b). For $kT \gg \hbar\omega_z$,

$$1/T_{1D} \propto T. \tag{2}$$

The Raman process involves pairs of phonons whose frequencies differ by ω_z. The assumed frequency dependence of the strain certainly does not hold for phonons near the Debye limit; however, using the assumption for the sake of simplicity, the Raman relaxation time is found in first-order perturbation to be given by

$$1/T_{1R} \propto (T/\theta)^7 J_6(\theta/T), \tag{3}$$

where θ is the Debye temperature of the lattice and the J function is a tabulated[12] transport integral. This form results from an integration over pairs of phonons of equal energies. The corresponding diagram is shown in Fig. 3(b). For T very much less than θ, $1/T_{1R}$ is proportional to T^7; for T greater than θ, $1/T_{1R}$ is proportional to T^2.

Equation (3) applies when the spin-lattice interaction is magnetic (e.g., via an electron-nuclear hyperfine coupling). If the dominant coupling is via the crystalline electric field and the spin-orbit interaction, the appropriate expression for T_{1R} of a one-electron system is[7,8]

$$1/T_{1R} \propto (T/\theta)^9 J_8(\theta/T). \tag{4}$$

This relation follows from second-order perturbation theory using the spin-lattice interaction terms linear in the strain. The appropriate diagram is shown in Fig. 4(b).

C. Cross Relaxation

All of the spin-relaxation mechanisms discussed above involve a system of isolated centers and lattice vibrations. A spin system may also relax by transferring its Zeeman energy to another system of spins. This process, known as cross-relaxation,[13] involves (a) spatial and usually spectral diffusion of Zeeman energy from one spin system to the other, and (b) spin-lattice relaxation of the spins which are acting as the energy sink. The diffusion steps are expected to be temperature-independent, while the spin-lattice relaxation will probably take one of the forms discussed above.

The temperature dependence of any observable cross-relaxation will be essentially determined by the step which is the bottleneck for the process. The identity of this step may change as the temperature is varied, giving a different dependence on temperature in the different temperature ranges. At high temperatures, the diffusion is expected to be the limiting step and the process independent of T.

D. Influence of a Light-Mass Defect on the Vibrational Spectrum

When an atom of a crystal is replaced by a lighter atom, the normal modes of the lattice are perturbed. It is possible to have a normal mode with a frequency greater than the maximum frequency for the unperturbed lattice. The amplitudes of motion of the neighboring particles at this frequency decrease exponentially with distance from the defect atom.[6] The higher the frequency of this mode with respect to the maximum of the unperturbed lattice, the more localized is the motion. Local modes associated with defect atoms in sites with cubic symmetry are triply degenerate.

Because of the localization, the strain at the defect associated with the local mode is larger than that in any of the band modes. The enhancement of the strain at the defect increases with increasing localization of the mode and would approach a limiting value of $p^{1/2}$ where p is the ratio of the number of atoms in the crystal to the number of atoms involved in the local mode. This large a factor will not be realized in practice owing to anharmonic effects.

In addition, the strain at the defect atom due to each band mode is reduced from the strain that would have been associated with a normal atom in a perfect lattice at that frequency.

E. Relaxation by Altered Band Modes

It can be shown for a light substitutional defect in a cubic lattice that the strain at the defect is still proportional to frequency for sufficiently low phonon frequencies, but decreases with increasing frequency near the Debye limit. The temperature dependence of the direct processes is the same as discussed above for a perfect lattice. At sufficiently low temperatures, the Raman processes also have unaltered temperature

[12] W. M. Rogers and R. L. Powell, Natl. Bur. Std. (U.S.) Circ. 595 (1958).

[13] N. Bloembergen, S. Shapiro, P. S. Pershan, and J. O. Artman, Phys. Rev. **114**, 445 (1959).

dependences, as given by Eqs. (3) or (4). However, the reduction in the strain near the Debye limit causes the approach to T^2 dependence to set in at lower temperatures than those for Eqs. (3) and (4). Because the transition probabilities for the Raman processes are sums over the whole range of lattice frequencies the temperature dependence may not be distinguishable from that expected for the unaltered lattice.

F. Relaxation by Local Modes

We now consider the processes of Figs. 2(a), 3(a), 4(a), and 5(a) when local modes are involved in the relaxation. We again consider the expansion in terms of cubic anharmonicity. With the magnetic fields available, the process 2(b) has zero probability of occurring since it uses harmonic phonons. The processes 3(b) and 4(b) cannot conserve energy either. In Fig. 5 we illustrate a relaxation process involving the cubic spin-lattice interaction. Note that if the local-mode frequency is less than twice the Debye frequency, process 5(b) will have a finite probability.

The transition probability for the direct process of Fig. 2(a) will presumably be very small for a reasonably sharp local mode. The other processes that we have diagrammed will show a distinctive temperature dependence if they involve a local mode whose frequency is well separated from the band frequencies. The first nonvanishing contribution to Raman scattering of local modes involves the coupling of two band modes via the cubic anharmonicity. Figure 3(c) illustrates one of the transitions in this process. Some of these terms were omitted in the previous discussion.[3]

The second-order matrix element appropriate to Fig. 3(c) is

$$\sum_q \frac{\langle r|K\epsilon^3 l_0^3|q\rangle\langle q|V_2\epsilon^2 l_0^2|p\rangle}{E-E_q}, \tag{5}$$

where $E=E_p=E_r$, K is the cubic anharmonicity coefficient, V_2 is one half of the second derivative with respect to displacement of the spin-lattice interaction, and l_0 is the equilibrium particle separation. The strain at the defect can be expressed as

$$\epsilon=\textstyle\sum_k S_k(a_k^\dagger+a_k), \tag{6}$$

where S_k is the strain per quantum in the mode k of the defect lattice and the sum is taken over all the modes.

The largest contribution to Eq. (5) comes from the terms involving any one of the triply degenerate local modes in the intermediate state. We can represent the occupation numbers for each of the three degenerate local modes by $N_x(\omega_L)$, $N_y(\omega_L)$, and $N_z(\omega_L)$. In the case that the intermediate state involves the same local mode as the initial state the temperature dependence of the spin-lattice relaxation is given by Eq. 7(a). If the intermediate state involves one of the other degenerate local modes, the temperature dependence is given by Eq. 7(b)

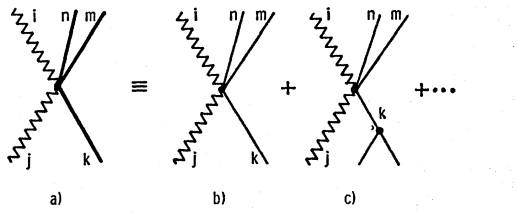

FIG. 5. Diagrams representing spin-lattice interactions cubic in strain. The symbolism is the same as in Fig. 2.

$$\langle N_\alpha^3(\omega_L)\rangle\langle N(\omega_1)+1\rangle\langle N(\omega_2)+1\rangle, \tag{7a}$$

$$\langle N_\alpha(\omega_L)\rangle\langle[N_\beta(\omega_L)+1]^2\rangle\langle N(\omega_1)+1\rangle\langle N(\omega_z)+1\rangle. \tag{7b}$$

Energy conservation in these transitions obviously requires the frequency of the local mode ω_L to be no more than twice the Debye frequency ω_D. We neglect ω_z. The temperature dependence of both of these processes reduces to a simple form for a range of values of ω_L. When kT is much less than $\hbar\omega_D$ and also much less than $\hbar(\omega_L-\omega_D)$, then the occupation numbers of all modes of interest in 3(c) can be written as

$$N(\omega)=\exp(-\hbar\omega/kT)\ll 1. \tag{8}$$

In this limit $\langle N^3(\omega)\rangle=\langle N^2(\omega)\rangle=\langle N(\omega)\rangle$ and the temperature dependences (7a) and (7b) reduce to $\exp(-\hbar\omega_L/kT)$.

The other terms in which two band mode phonons are annihilated and one local-mode phonon is created have the factor $\langle N(\omega_1)\rangle\langle N(\omega_2)\rangle\langle[N(\omega_L)+1]^3\rangle$ for the case where the final-state and intermediate-state local modes are the same. In the same low-temperature limit of (8), the factor becomes

$$\exp(-\hbar\omega_1/kT)\exp(-\hbar\omega_2/kT),$$

which by energy conservation is

$$1/T_1\propto\exp(-\hbar\omega_L/kT). \tag{9}$$

Similar reasoning leads to the same temperature dependence for the relaxation processes illustrated in other figures, such as Figs. 4(c) and 5(b). So the local mode can effect an exponential temperature dependence by several different relaxation processes. We will make no effort in this paper to distinguish between such processes.

G. Orbach Process

It should be noted that, when the paramagnetic center has one or more electronic states other than the two for the observed EPR transition whose energy splittings from the observed states lie within the vibrational spectrum of the lattice, the relaxation may be dominated by phonons whose energies are equal to one of those splittings. The process could either be resonant absorption, as in Fig. 2(b), or a scattering,

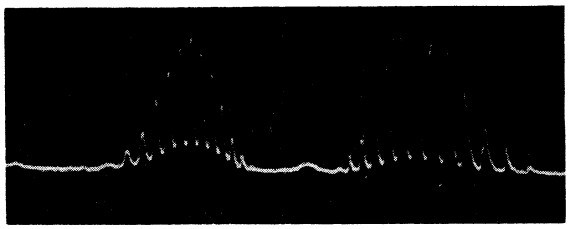

FIG. 6. EPR absorption spectrum of the atomic-hydrogen center in CaF_2 at 8.8 Gc/sec. The magnetic field is parallel to [110]; $T=4.2$°K. The abscissa is real time, and the field sweep is not linear with respect to time. The splitting between fluorine hyperfine components is 22 Oe; between proton components, 530 Oe.

as in Fig. 4(b). A simplified calculation gives[8,14,15] the temperature dependence to be

$$1/T_1 \propto [\exp(\Delta/kT)-1]^{-1} \quad (10)$$

for Δ the appropriate energy splitting. This "Orbach" process appears with an exponential dependence on temperature, as in (9), when Δ applies to an excited electronic state and $\Delta \gg kT$.

H. Summary

We note that these mechanisms of relaxation are assumed to be independent and that therefore their effects are additive. If the atomic hydrogen center in calcium fluoride is relaxed via hyperfine coupling, we expect to be able to describe the relaxation by

$$1/T_1 = BT + C(T/\theta)^7 J_6(\theta/T) + D\exp(-T_H/T), \quad (11)$$

where θ is an effective Debye temperature and $kT_H/\hbar$ is the frequency of a local mode associated with the hydrogen atom. The presence of a local mode may, in addition to generating the third term, influence: (a) the value of the coefficient B in the direct process term; and (b) the form of the term for the Raman process, lowering the effective Debye temperature in the J_6 function.

If the local mode involves motion of the paramagnetic center with respect to its surroundings, the frequency (ω_L) of the mode will depend on the mass of the center. The details of this dependence will involve the nature of the effective interatomic forces and the details of the motion. As an example, if the mode involves motion of only one atom moving in a harmonic potential, ω_L will be proportional to $M^{-1/2}$ where M is the mass of that atom.

If cross relaxation is present, we will represent it by adding a term of unspecified temperature dependence $\mathfrak{A}(T)$. Then the spin-relaxation time constant τ may be written

$$1/\tau = 1/T_1 + \mathfrak{A}(T). \quad (12)$$

Usually $\mathfrak{A}(T)=A$, independent of T.

[14] S. A. Al'tshuler, Sh. Sh. Boshkirov, and M. M. Zaripov, Fiz. Tverd. Tela 4, 3367 (1962) [English transl.: Soviet Phys.—Solid State 4, 2465 (1963)].

[15] D. E. McCumber, Phys. Rev. **130**, 2271 (1963).

III. EXPERIMENTAL TECHNIQUE

The samples were cleaved from single crystals of calcium fluoride. The crystals were obtained from the Harshaw Chemical Company or were grown by seed pulling in a controlled atmosphere furnace in our laboratory. The atomic-hydrogen centers were produced by the techniques described by Hall and Schumacher.[1] The crystals were annealed in hydrogen, at a pressure of 100 Torr for several hours at 650°C. It was found necessary to have the crystals in contact with aluminum during the anneal. The role played by the aluminum is obscure. After annealing, the crystals were subjected to a dose of about 10^7R of 0.5-MeV gamma rays. The resulting concentrations of atomic hydrogen were of the order of 10^{18} cm^{-3}.

The relaxation times were measured by the field-sweep inversion recovery technique which has been described elsewhere.[16] The net magnetization of the spin system was reversed by field-sweep adiabatic rapid passage and the return to equilibrium of the system is monitored. Measurements were made at a frequency of about 9 Gc/sec. Small Helmholtz coils mounted on a sample cavity were used to sweep the field through the

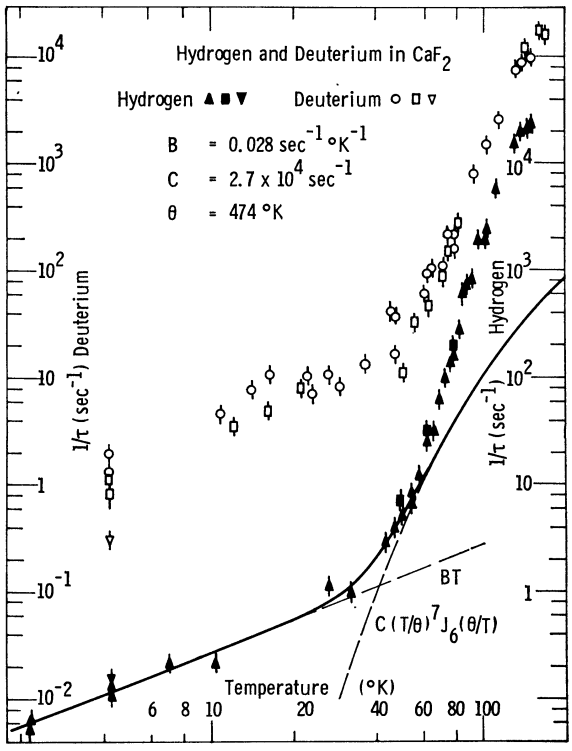

FIG. 7. Reciprocal of relaxation time versus temperature observed for atomic hydrogen and atomic deuterium in CaF_2 at 8.8 Gc/sec. Both scales are logarithmic. The samples denoted by triangles and circles were prepared from Harshaw crystals; the squares denote crystals grown in our laboratories. Note that the vertical scale for deuterium is shifted one decade with respect to the hydrogen scale.

[16] J. G. Castle, Jr., D. W. Feldman, P. G. Klemens, and R. A. Weeks, Phys. Rev. **130**, 577 (1963).

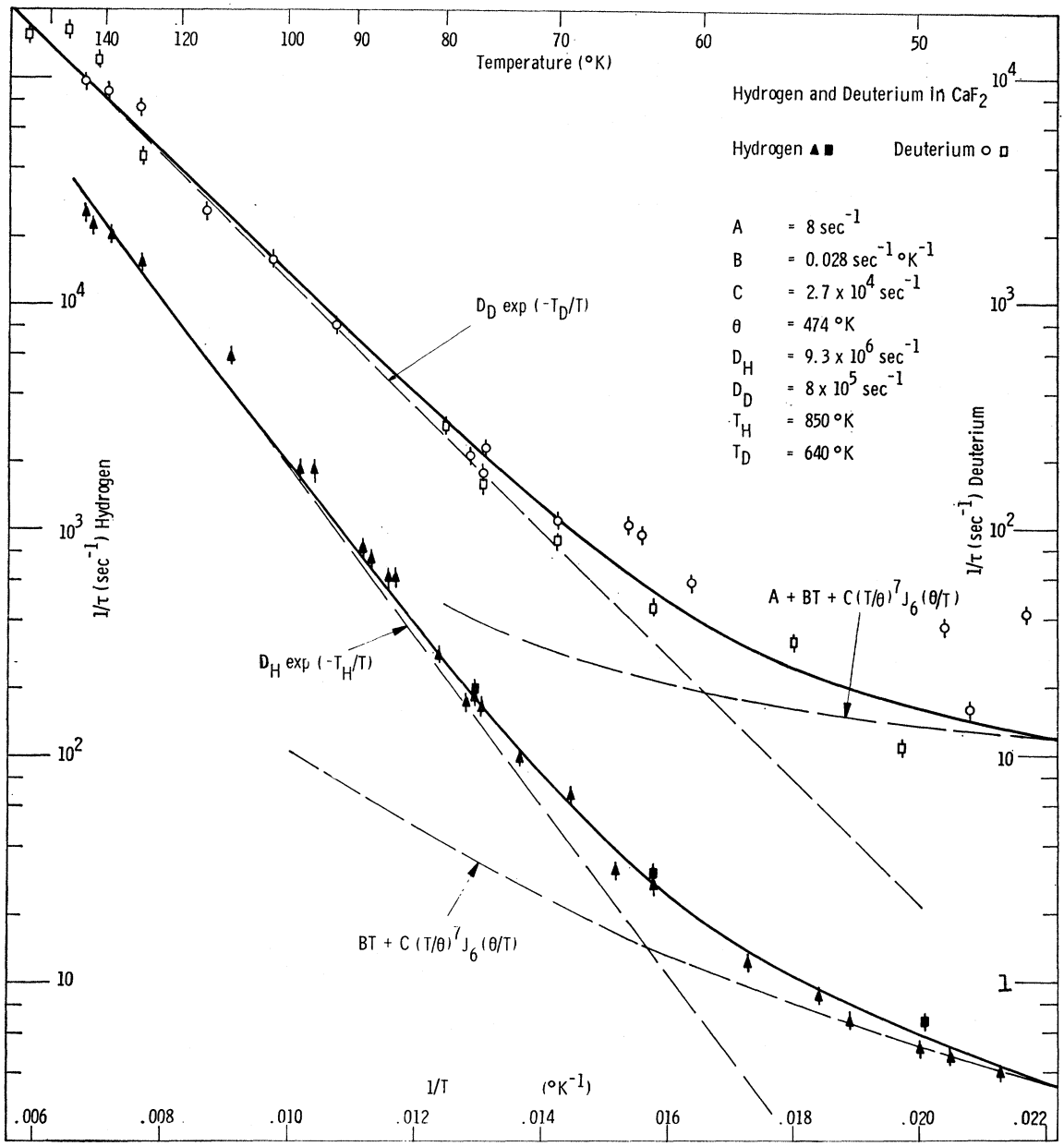

FIG. 8. Reciprocal of relaxation time versus temperature for atomic hydrogen and atomic deuterium in CaF_2. Note that the vertical scale for deuterium is shifted one decade from that for the hydrogen. Note also that the abscissa is linear in $1/T$.

desired resonance lines in a time short compared to the relaxation time being measured. A 5-W pulse of 9-Gc/sec radiation could be turned on during any selected part of the field sweep to invert any desired portion of the spectrum. The temperature of the sample was monitored by thermocouples which were frequently calibrated at the boiling points of helium and nitrogen.

IV. RESULTS FOR HYDROGEN

Figure 6 shows the appearance of the absorption spectrum of atomic hydrogen in calcium fluoride.[1] The magnetic field is parallel to the [110] direction of the crystal. The two groups of thirteen lines in Fig. 6 correspond to the two possible values of m_I of the proton spin. The well-resolved lines in each group are due to the hyperfine coupling of the electron to the surrounding fluorine nuclei.

It should be noted that an additional resonance appears at a g value of approximately 2.00. This resonance was always produced in the process of generating hydrogen centers. The absorption in this resonance relative to that of the hydrogen centers varied from sample to sample, often being comparable. The presence

of a weak resonance at $g=2$ was noted by Hall and Schumacher.[1]

Various experiments were carried out in which a selected portion of the spectrum was perturbed. It was found at 4.2°K that the sets of absorption lines corresponding to the two orientations of the proton moment relaxed independently. In the discussion below this independence will be interpreted as evidence that modulation by the phonons of the hyperfine coupling to the proton is not the mechanism responsible for the electron spin relaxation.

In principle the same procedure could be used to determine the role in the relaxation process of the hyperfine coupling to the fluorine nuclei. In practice this is more difficult because of the overlap of adjacent fluorine hyperfine components and has not as yet been done.

Figures 7 and 8 show the temperature dependence of the measured spin relaxation time of atomic hydrogen centers in calcium fluoride from 1.2 to 200°K. Data were taken for four samples prepared independently from different source crystals but only three are represented in the figures. Two of the samples, labeled ▲ and ▼, gave the same longest value of τ at 4.2°K. For $T\leq 30$°K, the values for the ▲ sample are accurately given in sec^{-1} by

$$1/\tau=2.8\times10^{-2}T. \quad (13)$$

For the sample ▼ the only other relaxation measured was that of the deuterium lines at 4.2°K. The other two samples had appreciably smaller values of τ below 50°K than the ▲ sample, and therefore they were not plotted. At temperatures above 50°K there is good agreement in the value of τ measured for two samples, as shown. The fourth sample was observed to have the same relaxation times as the values shown from 40 to 97°K. For temperatures above 30°K, the observed relaxation is clearly faster than that predicted by (13). The excess relaxation over the values expected from (13) can be accurately fitted in the range up to 75°K by any of several functions and in the range above 75°K by the expression

$$1/\tau=9\times10^{6}\exp(-850/T). \quad (14)$$

Relaxation at temperatures between 30 and 75°K is faster than that predicted by the sum of (13) and (14). The excess over (13) and (14) can be well fitted by a term of the form

$$(T/\theta)^{7}J_{6}(\theta/T), \quad (15)$$

but these data do not cover a sufficient range of T to permit specification of a unique value for θ. The largest value allowed by these data is approximately θ_D, the value of the Debye temperature determined by specific-heat measurements.[17] The solid curve in Fig. 8 is the sum

$$1/\tau=BT+C(T/\theta)^{7}J_{6}(\theta/T)+D_H\exp(-T_H/T), \quad (16)$$

where θ was chosen to be 474°K in agreement with the specific heat Debye temperature,[17] $B=(2.8\pm0.3)10^{-2}$ sec^{-1} °K^{-1}, $C=(2.7\pm0.3)10^{-4}$ sec^{-1}, $D_H=(9\pm2)10^{6}$ sec^{-1}, and $T_H=850\pm60$°K.

Other descriptions of the data above 50°K were attempted. These data cannot be fitted satisfactorily by using the specific heat for the Debye limit in expressions (3) or (4) for the Raman processes.

The relaxation time for the mystery resonance near $g=2$ was measured to be about 1 sec at 4.2°K. The relaxation time was observed to be about twice as long at 2.1°K. Measurements at higher temperatures were not made on this line. It was also found that there was no appreciable cross relaxation between this line and the hydrogen lines.

V. RESULTS FOR DEUTERIUM

Samples containing atomic deuterium were prepared in a manner similar to that described above for hydrogen. The EPR spectrum of deuterium is much more complex in appearance than that of hydrogen. Because of the smaller moment of the deuterium nucleus the three groups of lines corresponding to different orientations of the deuteron moment are not resolved. The appearance of the deuterium resonance was such that the resonance at $g=2.0$, which was observed in all hydrogenated samples, would have been hidden.

Figures 7 and 8 show the results of spin-relaxation measurements for atomic deuterium in several samples. In both figures the vertical scales have been shifted for one decade from those for hydrogen to permit visual discrimination.

At 4.2°K, the three samples had significantly different relaxation times, faster than the hydrogen value by factors from 3 to 30. For the one labeled ○ the longer of the two relaxation times was observed 18 months after the shorter one; at 48°K the same effect of an 18-month wait was observed in the same sample. From 4 to 45°K, the relaxation time decreases slowly tending toward temperature independence above 20°K at 0.12 sec. The same data might be fitted by $1/\tau=0.4T$.

For $T>75$°K, the excess of $1/\tau$ over 8 sec^{-1} is accurately given by

$$1/\tau\propto\exp(-T_D/T). \quad (17)$$

There is, as can be seen in Figs. 7 and 8, observed relaxation in excess of that expected from (17) plus 8 sec^{-1} for the intermediate temperatures. This excess for intermediate T is satisfactorily given by a term, $(T/\theta)^{7}J_{6}(\theta/T)$, identical to that used in (16) for the atomic hydrogen center. Therefore, the relaxation time observed for atomic deuterium centers at 8 kOe is

[17] *American Institute of Physics Handbook* (McGraw-Hill Book Company, New York, 1957), pp. 4–47.

accurately given by

$$1/\tau = A + BT + C(T/\theta)^7 J_6(\theta/T) + D_D \exp(-T_D/T), \quad (18)$$

where $A = 8 \pm 2$ sec^{-1}, $D_D = (8 \pm 2)10^5$ sec^{-1}, $T_D = 640 \pm 80$°K and the other parameters are the same as for hydrogen. Approximately the same fit is obtained if the terms $A+BT$ are replaced by $0.4T$.

VI. DISCUSSION OF RESULTS

The principal feature discussed in this paper is the exponential character of the temperature dependence observed for the atomic hydrogen and deuterium centers at temperatures above 75°K. We first consider the question of whether the observed relaxation times are intrinsic to these electron-lattice systems. We then discuss those values that appear to be intrinsic in terms of normal relaxation processes dominant at the lower temperatures. After predicting from this the relaxation expected at the higher temperatures, likely sources of the unusual temperature dependence are described.

A. Intrinsic

Above 50°K the values of τ measured in several samples using crystals from different sources agree to within approximately the statistical uncertainty of each point, both for hydrogen and for deuterium. These values are therefore assigned as the intrinsic T_1 for the isolated centers.

Below 50°K there is an appreciable disparity between the values of measured for the several samples, both for those containing hydrogen and for those containing deuterium. However, one hydrogen sample had $1/\tau \propto T$ below 30°K. This same sample also had the slowest relaxation at each temperature except at 4.2°K where the same value was found in another sample. Therefore this set of τ values is labeled as the T_1 values intrinsic to the atomic hydrogen center.

Below 50°K, relaxation in every deuterium sample was observed to be faster than that of the hydrogen center. Since the proton moment is observed to play no role in relaxing hydrogen centers at the lowest temperatures, the mechanism of relaxation is either via hyperfine coupling to the fluorine nuclei or via orbit lattice interaction. In either case the deuterium center should have the same transition probabilities for the direct and Raman processes as the hydrogen center does. It is on the basis of this reasoning and not on direct experimental evidence that the expressions fitting the deuterium data include terms for the direct and Raman processes that are identical to those for the hydrogen center.

The added relaxation observed for deuterium centers below $T = 50$°K may be due to cross relaxation to the spin system responsible for the mystery line at $g = 2.00$ since at 4.2°K the observed in each deuterium sample is within a factor of 4 of the value measured for that line in one of the hydrogen samples. Cross relaxation to this unknown spin system, probably vacancy centers similar to F centers, is expected to be more effective for deuterium than for hydrogen at equal densities because of the superposition of the spectra in the case of the deuterium. Therefore, the values observed for deuterium below 50°K are attributed to cross relaxation. On this basis, the τ observed to be 0.12 sec from 15 to 35°K should apply to the cross-relaxation process at all higher temperatures.

With independent transition probabilities, relaxation from the several intrinsic and cross-relaxation processes are additive at each temperature. It is necessary, therefore, to estimate the extent to which the processes which dominate the relaxation at low temperatures contribute to the relaxation at the highest temperatures. To do this, we use the data taken below 75°K and the information known about the hydrogen centers' equilibrium configuration to construct the skeleton of a relaxation model for the hydrogen center.

B. The Atomic Hydrogen Center at Low Temperatures

The data for hydrogen in the sample having the longest τ below 30°K are consistent with a direct process and Eqs. (2) and (13) become $1/T_1 = 2.8 \times 10^{-2} T$, assuming the data to be intrinsic to the isolated center. Above 30°K relaxation varies more rapidly with temperature. Normally this is due to Raman scattering processes. A model for the Raman processes should be based on the following: (1) The g value of the center is essentially that of the free atom.[1] (2) The optical splittings[18] of the center are probably at least as large as the band gap of CaF_2. (3) The hyperfine coupling of the center to its surrounding nuclei is rather large,[1] and we find that the proton moment does not contribute significantly to the center's relaxation at the lowest temperatures. (4) Experiments in alkali halides[19,20] indicate the Raman processes for electron-spin relaxation are due to hyperfine coupling and are accurately described by the term $(T/\theta)^7 J_6(\theta/T)$, as in Eq. (15), with $\theta = \theta_D$ as determined by specific-heat data. (5) Calcium fluoride is found to obey the simple Debye specific-heat law.[21]

From assumptions (1) and (3), the most likely candidate for spin-lattice coupling becomes the electron-fluorine hyperfine interaction. Therefore, with (4) and (5), the form expected for the Raman processes is that of Eq. (15). The modification of the lattice vibrations due to the light mass should, according to Sec. IIE, cause the value of the effective limit θ to be lower than θ_D. We are therefore overestimating the contribution

[18] G. Baldini, Phys. Rev. **136**, A248 (1964).
[19] D. W. Feldman, R. W. Warren, and J. G. Castle, Jr., Phys. Rev. **135**, A470 (1964).
[20] M. J. Weber, Phys. Rev. **130**, 1 (1963).
[21] M. Blackman, *Encyclopedia of Physics*, edited by S. Flügge (Springer-Verlag, Berlin, 1955), Vol. VII, p. 329.

of the Raman processes at the highest temperatures when we use $\theta=\theta_D$ in the term of the form of Eq. (15).

It should be noted that one function which does fit the relaxation data in Fig. 7 rather well above 50°K is the form $(T/\theta)^9 J_6(\theta/T)$, discussed in Sec. IIB, but with $\theta=1200$°K. This fit to the data is judged to be spurious on the grounds that such a high value for the effective upper limit of the lattice spectrum is unreasonable. The specific-heat value of θ_D is 474°K.

No electronic excited level of the atomic-hydrogen center exists within the vibrational spectrum of the lattice, according to assumption (2). So we expect the relaxation of the atomic-hydrogen center to contain the following components:

$$BT+C(T/\theta)^7 J_6(\theta/T), \tag{19}$$

where the coefficients are fixed by the relaxation data taken below 60°K, and θ is not greater than the usual Debye limit θ_D.

C. The Atomic Hydrogen Center at Higher Temperatures

The data taken above 75°K are rather well fitted, as in Fig. 8, by an exponential term of the form given in Eq. (9). When the components of Eq. (19) are subtracted, the remaining relaxation is accurately given down to 60°K by the term $D_H \exp(-T_H/T)$ with $T_H=850\pm60$°K. This value is larger than any reported[22] for optical modes of CaF_2.

Relaxation via local modes is suggested as the source of this term. According to the discussion in Sec. II, the presence of local modes of vibration at the site of the spin center can lead to spin-lattice relaxation with this temperature dependence by any of several specific processes. The frequency of any local mode involving the motion of the hydrogen atom and therefore the activation temperature should change upon substitution by deuterium.

D. The Atomic-Deuterium Center

The relaxation data above 50°K has been judged to be intrinsic to the isolated atomic deuterium center. It is clear in Fig. 8 that from liquid-nitrogen temperatures up the measured times are accurately given by

$$1/T_1=D_D \exp(-640/T). \tag{20}$$

Subtraction of the expected direct and Raman processes, as in Eq. (19), and the observed cross relaxation, from the data observed above 50°K, make Eq. (20) an excellent fit all the way. Therefore the activation temperature of 640±80°K is intrinsic to the atomic deuterium center in calcium fluoride.

[22] W. Kaiser, E. G. Spitzer, R. H. Kaiser, and L. E. Howarth, Phys. Rev. **127**, 1950 (1962).

E. Local Modes

The ratio of T_H to T_D is observed to be between 1.1 and 1.5. The fact that the activation temperature is sensitive to the mass M of the defect atom is taken as confirmation of the assignment of the observed effect to local modes.

In the harmonic approximation for the defect lattice, the frequency of a local mode, ω_L, is expected[6] to be independent of M for $\omega_L/\omega_D\approx1$, and to vary as $M^{-1/2}$ for $\omega_L/\omega_D\gg1$. For a potential stronger than harmonic, the variation with M would be somewhat stronger. The harmonic approximation is consistent with the data but the amplitude of the motion of the hydrogen atom would be so large as to make this approximation questionable.

The ratio of the coefficients, D_H and D_D, determined from the data in Figs. 7 and 8 depends sharply on the activation temperature selected. Within the range of the data, D_H is between 5 and 20 times D_D. This trend is consistent with the expectation that the higher the frequency of a local mode the larger is the local strain.

VII. SUMMARY

The time constant with which an atomic-hydrogen center relaxes in the lattice of calcium fluoride at a temperature in the range of 70 to 165°K is observed to have an exponential temperature dependence. The activation temperature of 850°K is characteristic of the isolated center because the same values of τ are observed over this range in three different samples. Similar observations on crystals containing atomic deuterium show a characteristic activation temperature of 640°K.

From relaxation measurements at temperatures down to 1.2°K, tentative identification is made of the direct and Raman relaxation processes.

We conclude that the observed activation temperatures correspond to the energies of local modes involving the motion of the hydrogenic defect atom relative to its neighbors. Relaxation of the spin is accomplished by excitation of these local modes. We further suggest that the local strain generated by the local mode is quite large, as expected.

ACKNOWLEDGMENTS

We are indebted to P. G. Klemens for his original suggestion of the local-mode problem and for helpful discussions; to R. T. Schumacher for his stimulating suggestions, including the suggestion of calcium fluoride as a host, and for supplying several samples; to J. H. Parker, Jr., for growing crystals and preparing samples; and to M. Ashkin for some clarification of theoretical considerations.

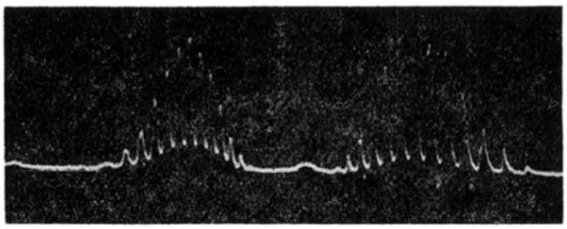

FIG. 6. EPR absorption spectrum of the atomic-hydrogen center in CaF_2 at 8.8 Gc/sec. The magnetic field is parallel to [110]; $T=4.2°K$. The abscissa is real time, and the field sweep is not linear with respect to time. The splitting between fluorine hyperfine components is 22 Oe; between proton components, 530 Oe.